metals

MDPI

Article

Influence of Thermal and Magnetic History on Direct ΔT_{ad} Measurements of $Ni_{49+x}Mn_{36-x}In_{15}$ Heusler Alloys

Luis M. Moreno-Ramírez [1], Antonio Delgado-Matarín [1], Jia Yan Law [1], Victorino FRANCO [1,*], Alejandro Conde [1] and Anit K. Giri [2]

[1] Dpto. Física de la Materia Condensada ICMSE-CSIC, Universidad de Sevilla, P.O. Box 1065, 41080 Sevilla, Spain; lmoreno6@us.es (L.M.M.-R.); antonio.delgado.matarin@gmail.com (A.D.-M.); jylaw@us.es (J.Y.L.); conde@us.es (A.C.)

[2] CCDC Army Research Laboratory, Aberdeen Proving Ground, MD 21005, USA; anit.k.giri.civ@mail.mil

* Correspondence: vfranco@us.es; Tel.: +34-954-553886

Received: 23 September 2019; Accepted: 23 October 2019; Published: 25 October 2019

Abstract: In the present work, using Heusler $Ni_{49+x}Mn_{36-x}In_{15}$ (with x = 0 and 0.5) alloys, it is shown that the choice of the appropriate measurement protocol (erasing the prior state of the sample in between experiments) in ΔT_{ad} first shot characterization is crucial for obtaining reliable results. Unlike indirect measurements, for which incorrect protocols produce overestimates of the characteristics of the material, erroneous direct measurements underestimate ΔT_{ad} in the region close to its first order phase transition. The error in ΔT_{ad} is found to be dependent on the temperature step used, being up to ~40% underestimation, including a slight shift in its peak temperature.

Keywords: magnetocaloric materials; direct ΔT_{ad} measurement; NiMnIn Heusler alloys

1. Introduction

Magnetic materials, when adiabatically subjected to magnetic field changes, can undergo significant adiabatic temperature change (ΔT_{ad}) ascribed to the magnetocaloric (MC) effect [1–3]. This effect constitutes the basis of magnetic refrigeration, an emergent environmental-friendly refrigeration alternative (50% more energy efficient than conventional systems) [4]. Nowadays, the basic study and optimization of MC materials and devices is a hot topic for the scientific community [5–7]. The maximum MC response is obtained close to a thermomagnetic phase transition, either first- (FOPT) or second-order (SOPT), being this a common criterion categorizing the materials. In the former case, it corresponds to a discontinuity in the first derivative of the free energy (with phase coexistence during the transition and hysteretic behavior) while a SOPT is associated to a discontinuity in the second derivative of the free energy (in this case, its resultant phase variation is continuous and reversible) [8]. To date, there are several promising MC materials being considered. Historically, Gd was the first material to demonstrate that magnetic refrigeration can serve as a real alternative to the conventional refrigeration systems though its high price and limited availability impeded further advances in commercialization of magnetic refrigerators [9]. Nowadays, there are other well-regarded MC material candidates with large MC responses that can surpass that of Gd, which include $Gd_5(Si,Ge)_2$ [10], MnFe(P,As) [11,12], $La(Fe,Si)_{13}$ [13,14], or Heusler alloys [15–18]; all of them belong to the FOPT type.

Hence, the appropriate performance evaluation is crucial for MC materials as that would determine their suitability for their technological application [19]. For FOPT MC materials, temperature and field variations are irreversible due to the intrinsic hysteresis of the transition [20,21]. This implies that the

partial transformation of the sample from previous measurement conditions could persist for subsequent measurements within its hysteretic range. This has been brought up when performing the continuous measurements for the indirect MC determination of the isothermal entropy change (ΔS_{iso}) as spurious peaks are found [22,23]. Therefore, it is important to consider the effects of partial transformations after each measurement and erase them to obtain physically meaningful data (usually termed as discontinuous protocols). This is made by cooling/heating well below/above the transition before proceeding to the next measurement. This process is also accompanied with an appropriate value of the magnetic field (depending on the particular phase to be stabilized). It should be stressed that these protocols refer to a first shot characterization to obtain information about the material's nature, however, it can be also evaluated in cycled conditions to examine the technological capacities [24,25].

In this work, the effect of the different measurement protocols on the direct ΔT_{ad} measurements is studied for two polycrystalline Heusler alloys (nominal compositions $Ni_{49}Mn_{36}In_{15}$ and $Ni_{49.5}Mn_{35.5}In_{15}$) exhibiting martensitic (FOPT) and Curie (SOPT) transitions (being a good test material for our purpose). We observe that ΔT_{ad} values can be severely underestimated when using continuous protocols instead of discontinuous ones, whereby discrepancies as high as up to 40% are observed in the region close to the martensitic transition. In addition, it is found that the protocol application becomes more crucial with increasing thermal hysteresis span as compared to the temperature step used in the measurements.

2. Methods

The direct MC effect of the samples was characterized using a direct ΔT_{ad} measurement system, whereby the sample chamber is maintained in vacuum (10^{-5} mbar) and its temperature is controlled by a Lake Shore Cryotronics temperature controller. The variable magnetic field generator is composed of two concentric Hallbach cylinders with a maximum magnetic field of 1.76 T. The temperature change of the sample produced by the application/removal of a magnetic field is registered using a type T thermocouple in differential configuration, with its reference weld located in contact with the sample holder. Due to their composition, type T thermocouples do not have a magnetic field-dependent response. The other weld of the thermocouple is located between two pieces of sample with rectangular shape. The different measurement protocols were automated using our in-house implemented software with appropriately adjusted PID (Proportional–Integral–Derivative) parameters for the temperature controller (to avoid thermal oscillations around the selected temperature).

3. Results and Discussion

The chosen alloys exhibit low-temperature martensite transforming to austenite at higher temperatures from both microstructural and magnetic observations. Further details of their synthesis, structural characterization, and magnetocaloric properties can be found in References [26,27]. Their temperature dependence of magnetization is shown in Figure 1a for which various magnetic phase transitions upon heating can be observed: a martensitic (martensite to austenite) transition (FOPT) followed by a Curie transition of the austenitic phase at higher temperatures (SOPT). It can be observed that small compositional changes can significantly affect the martensitic transition (in agreement with literature) [28]. With respect to direct ΔT_{ad} measurements, Table 1 shows the different discontinuous protocols used in this work to perform the direct measurements. In the case of continuous protocols, the samples are neither cooled down nor heated up to the end of the transformation after the measurement at a selected temperature. The protocols have been selected taking into account that the martensitic transition of the alloys is shifted to lower temperatures under an applied magnetic field (magnetic field stabilizes the austenitic phase) [15]. It can be noted that the characterization protocols used are in conjunction with those proposed for indirect MC measurements of FOPT MC materials.

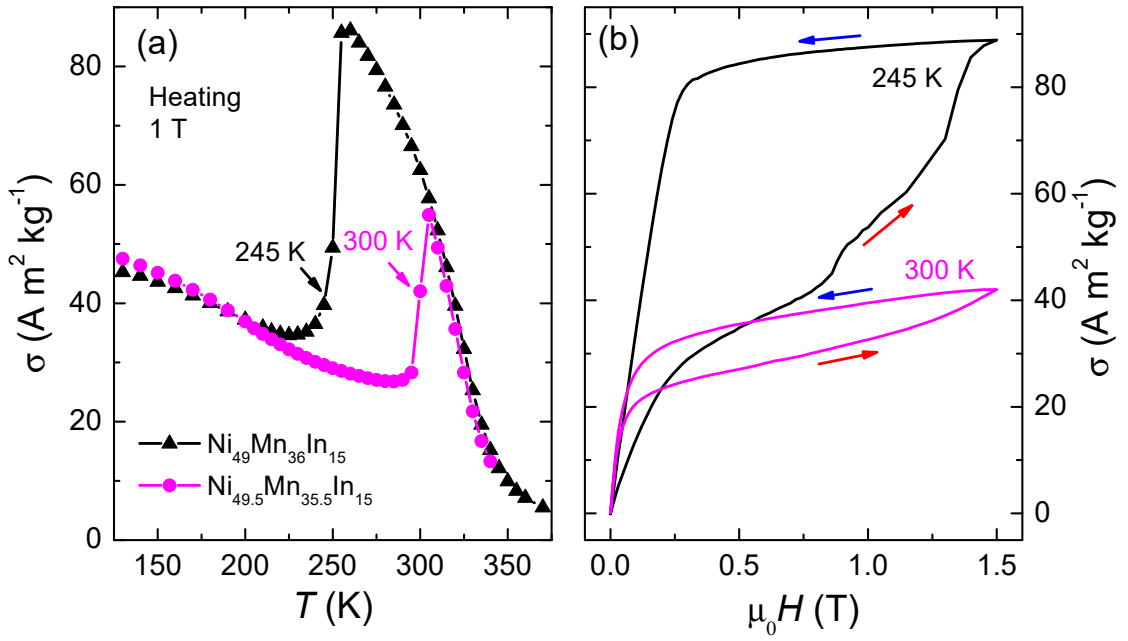

Figure 1. (**a**) Temperature dependence of magnetization of $Ni_{49}Mn_{36}In_{15}$ and $Ni_{49.5}Mn_{35.5}In_{15}$ samples measured at selected fields. (**b**) Magnetization/demagnetization curves at temperatures close to the martensitic transition.

Table 1. Heating and cooling discontinuous protocols on erasing the sample's history used in this work.

Heating	Cooling
Set the temperature well below the martensitic transition at low field	Set the temperature well above the martensitic transition at high field
Set the desired measurement temperature	Set the desired measurement temperature
Measure ΔT_{ad} from low to high field	Measure ΔT_{ad} from high to low field
Repeat the steps before measurement at a different temperature	Repeat the steps before measurement at a different temperature

The temperature dependence of ΔT_{ad} at 1.76 T while cooling using discontinuous (i.e., erasing the memory of the sample between measurements) and continuous (i.e., not erasing it) measurement protocols with a temperature step of 5 K for $Ni_{49.5}Mn_{35.5}In_{15}$ sample is shown in Figure 2. Two peaks are clearly observed, which correspond to the martensitic and Curie transitions (around 295 K and 320 K, respectively). The former response is larger than the second one, although it happens in a narrower temperature range (as expected from the characteristics of each transition, i.e., an abrupt change for FOPT and a gradual change for SOPT). A magnetic field sweep rate of 0.5 T s^{-1} was selected for both samples. The discontinuous protocol was applied by subjecting the sample to a reset temperature of 350 K and 1.76 T (which is well above its martensitic transition of ~295 K). Error bars correspond to the precision of the system (close to room temperature ≈ 0.06 K). The different ΔT_{ad} results of $Ni_{49.5}Mn_{35.5}In_{15}$ show slight differences for the two measurement protocols in the region close to the martensitic transition while in the region close to the ferro-paramagnetic transition there are no differences. This is further magnified in the inset of Figure 2 using the temperature dependence of $\delta\Delta T_{ad}$ (where $\delta\Delta T_{ad} = \Delta T_{ad}$ (continuous) − ΔT_{ad} (discontinuous)), however, the error bars avoid any detailed discussion. In addition, similar features are observed for the ΔT_{ad} results using both protocols while heating (not shown).

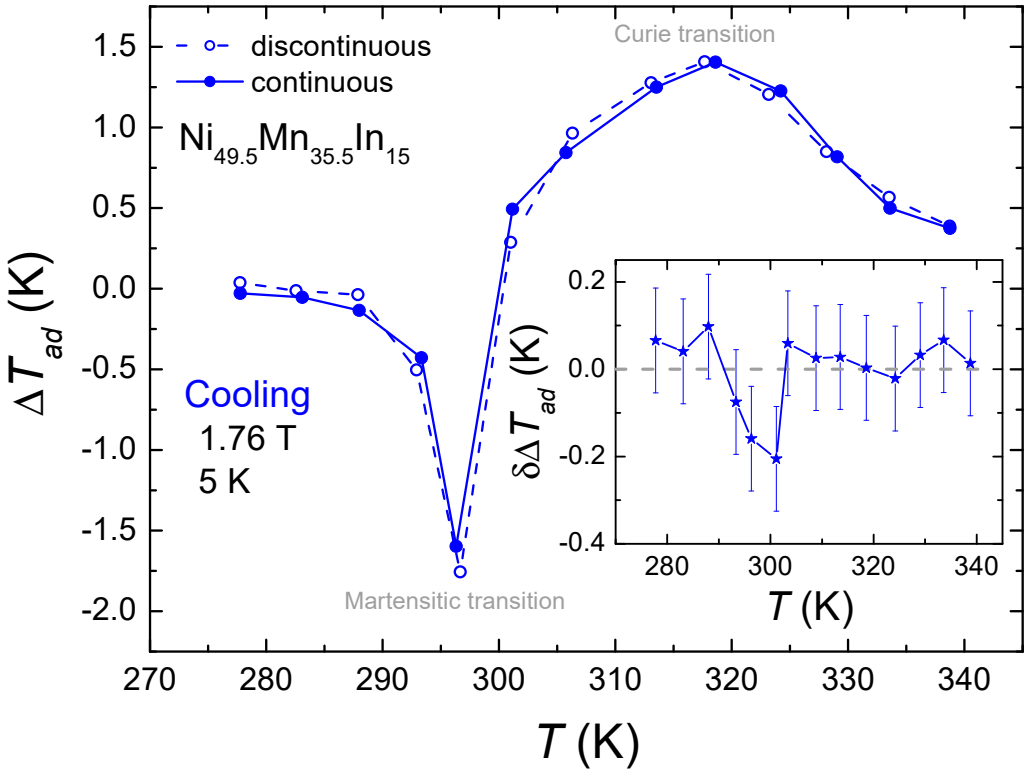

Figure 2. Temperature dependence of the adiabatic temperature change (ΔT_{ad}) of $Ni_{49.5}Mn_{35.5}In_{15}$ sample using discontinuous and continuous cooling protocols (open and solid symbols, respectively) with a temperature step of 5 K. Inset: differences between both ΔT_{ad} curves ($\delta\Delta T_{ad}$).

Figure 3 shows the temperature dependence of ΔT_{ad} at 1.76 T while heating using discontinuous and continuous measurement protocols with a temperature step of 5 K for $Ni_{49}Mn_{36}In_{15}$ alloy. In this case, the heating protocol was used with a reset temperature of 200 K and zero field, well below the martensitic transition around 260 K. For this sample, significant differences in the two curves with and without accounting for its history are observed (further magnified by $\delta\Delta T_{ad}$ in the inset of Figure 3). The ΔT_{ad} values associated to the martensitic transition are underestimated using the continuous protocol (maximum differences $\approx$ 20% are obtained around the peak temperature of ΔT_{ad}, T^{pk}), while the curves are relatively similar in the region close to the ferro-paramagnetic SOPT. In addition, the differences between their cooling $\Delta T_{ad}(T)$ curves using both protocols are also notable, in agreement to those observed from the heating protocol. To establish a comparison between both samples, it is important to note that the mass and shape of both samples are quite similar, in order to avoid the influence of these parameters in the general conclusions. With respect the hysteretic behavior, Figure 1b shows the magnetization/demagnetization curves at selected temperatures close to the martensitic transition for both samples. The hysteresis can be associated with the area enclosed between magnetization/demagnetization curves, being 50.2 and 9.6 A m^2 kg^{-1} T^{-1} for the $Ni_{49}Mn_{36}In_{15}$ and $Ni_{49.5}Mn_{35.5}In_{15}$, respectively. According to this, the magnetic hysteresis is larger for the $Ni_{49}Mn_{36}In_{15}$ sample, explaining why the differences between discontinuous and continuous protocols are more significant for this alloy (the discussion of the different hysteresis mechanisms is beyond the scope of this work). Furthermore, in agreement with the previous argument, the observed thermal hysteresis span between cooling and heating curves is larger for the $Ni_{49}Mn_{36}In_{15}$ sample than for the $Ni_{49.5}Mn_{35.5}In_{15}$ one, $\approx$12 and 6 K, respectively, which in the latter case is quite close to the selected temperature steps.

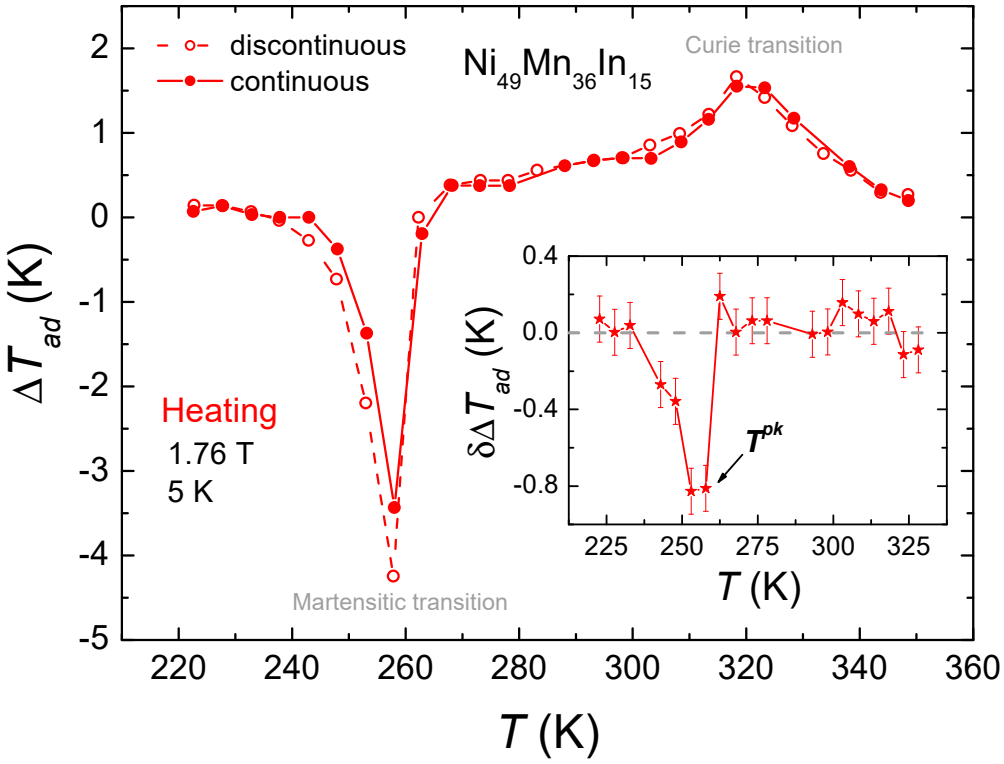

Figure 3. Temperature dependence of the adiabatic temperature change (ΔT_{ad}) of $Ni_{49}Mn_{36}In_{15}$ sample using discontinuous and continuous heating protocols (open and solid symbols, respectively) with a temperature step of 5 K. Inset: differences between both ΔT_{ad} curves ($\delta\Delta T_{ad}$).

To evaluate the influence of the temperature step on the direct measurements, a finer temperate step resolution of 2.5 K was used. It can be observed that the influence of the protocol on ΔT_{ad} while cooling becomes more significant near the martensitic transition of $Ni_{49}Mn_{36}In_{15}$ sample (for which the effects are more evident) with decreasing the temperature step (5 and 2.5 K are used for comparison), as shown in Figure 4. For the cooling protocol, a reset temperature of 350 K and a magnetic field of 1.76 T were chosen. The underestimation of ΔT_{ad} peak associated to martensitic transition increases to ~40% (a two-fold increase in comparison to the 5 K step measurements). With this finer resolution of the ΔT_{ad} curves, the peak temperature slightly shifts to higher temperatures when using continuous protocols. In addition, in the case of using discontinuous protocols (either for cooling or heating curves), the different ΔT_{ad} measured points are independent of the temperature step resolution, as expected.

It should be noted that, in contrast to the case of indirect ΔS_{iso} measurements, wherein an overestimation of the response is obtained when using continuous protocols, the effect on direct ΔT_{ad} measurements is a reduction of the response. This difference is due to the application of the Maxwell relation for determining ΔS_{iso}. The different fraction of phase transformation (due to a temperature variation) at the initial magnetic field, when compared to the one in an isofield curve, leads to an artificial increment of the magnetization change that produces a spurious spike in ΔS_{iso} data. In contrast, for ΔT_{ad} measurements, the deviations are ascribed to the irreversibility of the magnetization/demagnetization path which leads to a reduction of the transformed para-ferro fraction, reducing the ΔT_{ad} values. Using a finer temperature step, the differences of the amount of transformed fraction ascribed to the irreversibility increases as the number of measurements increase (each measurement contributing to the total amount of transformed phase), magnifying the error of the continuous protocol.

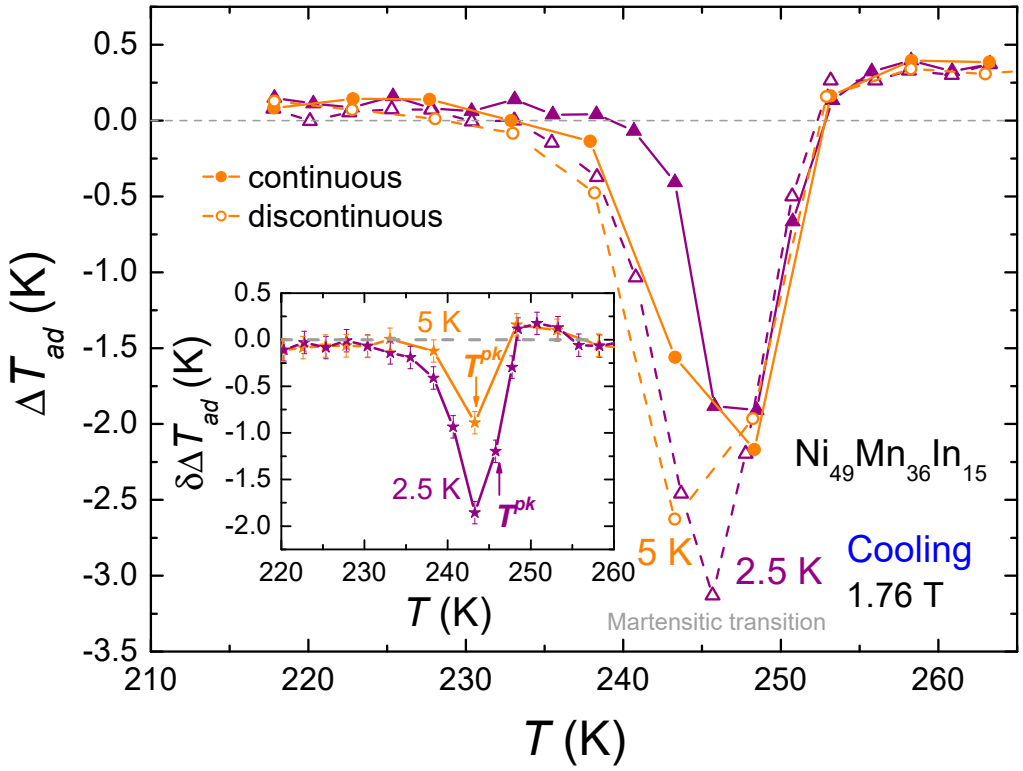

Figure 4. Temperature dependence of the adiabatic temperature change (ΔT_{ad}) of $Ni_{49}Mn_{36}In_{15}$ sample using discontinuous and continuous cooling protocols (open and solid symbols, respectively) with a temperature step of 2.5 and 5 K. Inset: differences between both ΔT_{ad} curves ($\delta\Delta T_{ad}$) using a temperature step of 2.5 and 5 K.

4. Conclusions

To conclude, the effect of the measurement protocols on the direct measurement of ΔT_{ad} has been studied using $Ni_{49+x}Mn_{36-x}In_{15}$ Heusler alloys (x = 0 and 0.5). For measurement protocols that do not take into account the history of the sample (i.e., continuous protocols), underestimations of ΔT_{ad} values were obtained in the region close to the martensitic FOPT, including a slight shift in its peak temperature. These errors in the measurement are shown to be highly dependent on the hysteretic temperature span with respect to the temperature step used for the measurements (discrepancies up to 40% are observed for the studied sample). Reducing the temperature step, instead of enhancing the reliability of the results, enhances the problem, which is counter-intuitive and relevant for designing appropriate characterization methods. This reduction of the experimentally measured ΔT_{ad} when a continuous protocol is used is in contrast with the overestimation of ΔS_{iso} when the history of the sample is also neglected. The results presented here clearly illustrate the importance of considering discontinuous measurement protocols to accurately determine the magnetocaloric response of FOPT materials even for direct methods.

Author Contributions: Conceptualization of the work by V.F., L.M.M.-R., A.C. and J.Y.L.; experimental measurements by L.M.M.-R. and A.D.-M.; data analysis by L.M.M.-R. and V.F.; samples provided by A.K.G.; writing of the manuscript by L.M.M.-R. and J.Y.L.; reviewed and edited by all the authors.

Funding: This work was supported by AEI/FEDER-UE (project MAT-2016-77265-R), the PAI of the Regional Government of Andalucía, and by the Army Research Laboratory under Cooperative Agreement Number W911NF-19-2-0212. A.K.G. acknowledges support from US Army Research Laboratory's Energy Coupled to Matter–Metals Program.

Acknowledgments: The views and conclusions contained in this document are those of the authors and should not be interpreted as representing the official policies, either expressed or implied, of the Army Research Laboratory

Conflicts of Interest: The authors declare no conflict of interest.

References

1. Lyubina, J. Magnetocaloric materials for energy efficient cooling. *J. Phys. D Appl. Phys.* **2017**, *50*, 053002. [CrossRef]
2. Gschneidner, K.A., Jr.; Pecharsky, V.K. Magnetocaloric Materials. *Annu. Rev. Mater. Sci.* **2000**, *30*, 387–429. [CrossRef]
3. Franco, V.; Blázquez, J.S.; Ipus, J.J.; Law, J.Y.; Moreno-Ramírez, L.M.; Conde, A. Magnetocaloric effect: From materials research to refrigeration devices. *Prog. Mater. Sci.* **2018**, *93*, 112–232. [CrossRef]
4. Zimm, C.; Jastrab, A.; Sternberg, A.; Pecharsky, V.; Gschneidner, K.; Osborne, M.; Anderson, I. Description and Performance of a Near-Room Temperature Magnetic Refrigerator. In *Advances in Cryogenic Engineering*; Kittel, P., Ed.; Springer: Boston, MA, USA, 1998; pp. 1759–1766.
5. Aprea, C.; Greco, A.; Maiorino, A. An application of the artificial neural network to optimise the energy performances of a magnetic refrigerator. *Int. J. Refrig.* **2017**, *82*, 238–251. [CrossRef]
6. Monfared, B.; Palm, B. Material requirements for magnetic refrigeration applications. *Int. J. Refrig.* **2018**, *96*, 25–37. [CrossRef]
7. Navickaitė, K.; Bahl, C.; Engelbrecht, K. Nature—Inspired Flow Patterns for Active Magnetic Regenerators Assessed Using a 1D AMR Model. *Front. Energy Res.* **2019**, *7*, 68. [CrossRef]
8. Callen, H.B. *Thermodynamics and an Introduction to Thermostatistics*, 2nd ed.; John Wiley & Sons: Hoboken, NJ, USA, 1985.
9. Brown, G.V. Magnetic heat pumping near room temperature. *J. Appl. Phys.* **1976**, *47*, 3673–3680. [CrossRef]
10. Pecharsky, V.K.; Gschneidner, K.A. Giant Magnetocaloric Effect in Gd5Si2Ge2. *Phys. Rev. Lett.* **1997**, *78*, 4494–4497. [CrossRef]
11. Yibole, H.; Guillou, F.; Zhang, L.; van Dijk, N.H.; Brück, E. Direct measurement of the magnetocaloric effect in MnFe(P, X)(X = As, Ge, Si) materials. *J. Phys. D Appl. Phys.* **2014**, *47*, 075002. [CrossRef]
12. Thanh, D.T.C.; Brück, E.; Trung, N.T.; Klaasse, J.C.P.; Buschow, K.H.J.; Ou, Z.Q.; Tegus, O.; Caron, L. Structure, magnetism, and magnetocaloric properties of MnFeP1−xSix compounds. *J. Appl. Phys.* **2008**, *103*, 07B318. [CrossRef]
13. Lyubina, J.; Gutfleisch, O.; Kuz'min, M.D.; Richter, M. La(Fe,Si)13-based magnetic refrigerants obtained by novel processing routes. *J. Magn. Magn. Mater.* **2009**, *321*, 3571–3577. [CrossRef]
14. Liu, J.; Moore, J.D.; Skokov, K.P.; Krautz, M.; Löwe, K.; Barcza, A.; Katter, M.; Gutfleisch, O. Exploring La(Fe, Si)13-based magnetic refrigerants towards application. *Scr. Mater.* **2012**, *67*, 584–589. [CrossRef]
15. Planes, A.; Mañosa, L.; Moya, X.; Krenke, T.; Acet, M.; Wassermann, E.F. Magnetocaloric effect in Heusler shape-memory alloys. *J. Magn. Magn. Mater.* **2007**, *310*, 2767–2769. [CrossRef]
16. Planes, A.; Manosa, L.; Acet, M. Magnetocaloric effect and its relation to shape-memory properties in ferromagnetic Heusler alloys. *J. Phys. Condens Matter* **2009**, *21*, 233201. [CrossRef] [PubMed]
17. Liu, J.; Gottschall, T.; Skokov, K.P.; Moore, J.D.; Gutfleisch, O. Giant magnetocaloric effect driven by structural transitions. *Nat. Mater.* **2012**, *11*, 620. [CrossRef]
18. Liu, J.; Scheerbaum, N.; Lyubina, J.; Gutfleisch, O. Reversibility of magnetostructural transition and associated magnetocaloric effect in Ni–Mn–In–Co. *Appl. Phys. Lett.* **2008**, *93*, 102512. [CrossRef]
19. Maiorino, A.; Del Duca, G.M.; Tušek, J.; Tomc, U.; Kitanovski, A.; Aprea, C. Evaluating Magnetocaloric Effect in Magnetocaloric Materials: A Novel Approach Based on Indirect Measurements Using Artificial Neural Networks. *Energies* **2019**, *12*, 1871. [CrossRef]
20. Gutfleisch, O.; Gottschall, T.; Fries, M.; Benke, D.; Radulov, I.; Skokov, K.P.; Wende, H.; Gruner, M.; Acet, M.; Entel, P.; et al. Mastering hysteresis in magnetocaloric materials. *Philos. Trans. Ser. A Math. Phys. Eng. Sci.* **2016**, *374*, 20150308. [CrossRef]
21. Ramírez, L.M.M. Methods for the Analysis of Thermomagnetic Phase Transitions of Magnetocaloric Materials. Ph.D. Thesis, Universidad de Sevilla, Sevilla, Spain, 12 July 2019.
22. Tocado, L.; Palacios, E.; Burriel., R. Entropy determinations and magnetocaloric parameters in systems with first-order transitions: Study of MnAs. *J. Appl. Phys.* **2009**, *105*, 093918. [CrossRef]

23. Kaeswurm, B.; Franco, V.; Skokov, K.P.; Gutfleisch, O. Assessment of the magnetocaloric effect in La,Pr(Fe,Si) under cycling. *J. Magn. Magn. Mater.* **2016**, *406*, 259–265. [CrossRef]
24. Gottschall, T.; Skokov, K.P.; Frincu, B.; Gutfleisch, O. Large reversible magnetocaloric effect in Ni-Mn-In-Co. *Appl. Phys. Lett.* **2015**, *106*, 021901. [CrossRef]
25. Gamzatov, A.G.; Aliev, A.M.; Ghotbi Varzaneh, A.; Kameli, P.; Sarsari, I.A.; Yu, S.C. Inverse-direct magnetocaloric effect crossover in Ni47Mn40Sn12.5Cu0.5 Heusler alloy in cyclic magnetic fields. *Appl. Phys. Lett.* **2018**, *113*, 172406. [CrossRef]
26. Zhou, L.; Mehta, A.; Giri, A.; Cho, K.; Sohn, Y. Martensitic transformation and mechanical properties of Ni49+xMn36–xIn15 (x = 0, 0.5, 1.0, 1.5 and 2.0) alloys. *Mater. Sci. Eng. A* **2015**, *646*, 57–65. [CrossRef]
27. Law, J.Y.; Díaz-García, Á.; Moreno-Ramírez, L.M.; Franco, V.; Conde, A.; Giri, A.K. How concurrent thermomagnetic transitions can affect magnetocaloric effect: The Ni49+xMn36-xIn15 Heusler alloy case. *Acta Mater.* **2019**, *166*, 459–465. [CrossRef]
28. Gao, B.; Hu, F.X.; Shen, J.; Wang, J.; Sun, J.R.; Shen, B.G. Tuning the magnetic entropy change of Ni50−xMn35+xIn15 alloys by varying the Mn content. *J. Appl. Phys.* **2009**, *105*, 083902. [CrossRef]